

Dynamic Scenario Representation Learning for Motion Forecasting with Heterogeneous Graph Convolutional Recurrent Networks

Xing Gao, Xiaogang Jia, Yikang Li, and Hongkai Xiong

Abstract—Due to the complex and changing interactions in dynamic scenarios, motion forecasting is a challenging problem in autonomous driving. Most existing works exploit static road graphs to characterize scenarios and are limited in modeling evolving spatio-temporal dependencies in dynamic scenarios. In this paper, we resort to dynamic heterogeneous graphs to model the scenario. Various scenario components including vehicles (agents) and lanes, multi-type interactions, and their changes over time are jointly encoded. Furthermore, we design a novel heterogeneous graph convolutional recurrent network, aggregating diverse interaction information and capturing their evolution, to learn to exploit intrinsic spatio-temporal dependencies in dynamic graphs and obtain effective representations of dynamic scenarios. Finally, with a motion forecasting decoder, our model predicts realistic and multi-modal future trajectories of agents and outperforms state-of-the-art published works on several motion forecasting benchmarks.

I. INTRODUCTION

Motion forecasting that predicts future trajectories of surrounding agents is an important and core module in autonomous driving systems for a safe and comfortable self-driving. Prediction is inherently uncertain and multi-modal. For example, a car may follow a vehicle ahead or change lanes on a congested road. Fortunately, historical trajectories of agents and high definition (HD) maps provide cues to perceive context information and render predictions feasible.

Exploitation of such information is nontrivial, however, because of (i) highly heterogeneous scenario components [1], including surrounding agents, lanes, traffic lights, *etc.*; (ii) complex and multiple interactions, like agent-agent interaction and agent-road interaction; (iii) interlaced spatio-temporal information, such as the trajectories of agents.

Several methods [2]–[6] rasterize the scenario to encode road information and historical trajectories of agents and exploit convolutional neural networks (CNNs) to learn complex interactions in the scenario. However, the sparse and irregular topology of road networks is inefficient to capture with rasterization-based representations and long-range interactions are difficult to process with local kernels of CNNs. Alternatively, a variety of graph-based methods [7]–[11] have been proposed recently. They typically employ graphs to represent irregular road networks and design various graph convolutional networks (GCNs) to further learn representations, such as VectorNet [7], LaneGCN [8], and LaneRCNN [9].

Xing Gao, Xiaogang Jia, and Yikang Li are with the Shanghai AI Lab, Shanghai 200232, China. (Corresponding author: Xing Gao, E-mail: gxyssy@163.com.)

H. Xiong is with the Department of Electronic Engineering, Shanghai Jiao Tong University, Shanghai 200240, China.

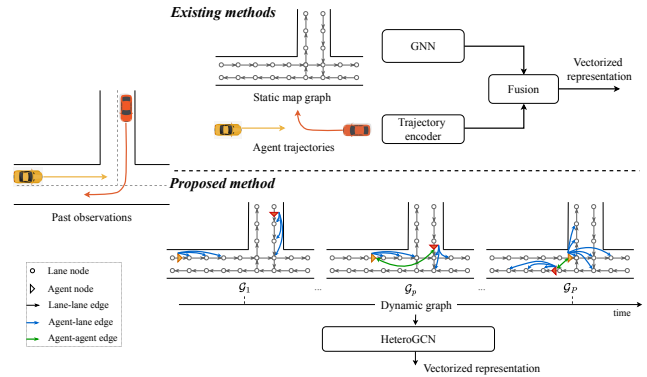


Fig. 1. A high-level demonstration of differences in dynamic scenario modeling and spatio-temporal information processing between existing methods and the proposed strategy.

However, these methods still have limitations in the following two aspects, as illustrated in Fig. 1. (i) Dynamic scenario modeling. Existing graph-based methods employ *static graphs* to model either road networks [8]–[10] or agent-agent interaction networks [11], instead of the whole scenario. These static homogeneous graphs fail to characterize the evolution in dynamic scenarios and the diversity of scenario components and their interactions. (ii) Joint spatio-temporal information processing. With static graph representation, existing methods typically process temporal dependencies and spatial interactions separately and combine them with late-fusion strategies. This will hinder the model from capturing the intrinsic correlation of spatio-temporal information.

To tackle these problems, we propose a novel dynamic scenario representation learning method for motion forecasting, called HeteroGCN, as illustrated in Fig. 2. HeteroGCN first models dynamic scenarios with the help of *dynamic heterogeneous graphs*. A heterogeneous graph convolutional recurrent network is further designed, which consists of heterogeneous graph convolution operators and motion encoding modules, for joint spatio-temporal information processing. The benefits of HeteroGCN are summarized as below.

- The proposed scenario modeling strategy explicitly encodes dynamic attributes of agents and multiple time-varying interactions in the scenario into the signal and topology of dynamic graphs, through mining from historical trajectories of agents, and inherits the advantages of static graph based road network encoding methods in capturing its sparse and irregular structure.
- The proposed graph convolutional recurrent net-

works gradually aggregate spatio-temporal information through processing the evolution of the topology and signal of dynamic graphs, which facilitates to explore intrinsic spatio-temporal dependencies.

- The designed heterogeneous graph convolution operator handles multiple types of nodes and interactions jointly yet differently, which permits to fuse road information and agent features at different time slots directly.

Based on the scenario representation, we predict future trajectories of agents with a motion forecasting decoder. It is shown to outperform state-of-the-art published motion forecasting methods on the challenging large-scale Argoverse and Argoverse2 motion forecasting benchmarks.

II. RELATED WORKS

We overview a collection of motion forecasting methods, especially focusing on vectorized (sparse) encoding based scenario representations.

Some early methods [12], [13] exploit LSTMs or GRUs to encode temporal information of agents but ignore spatial interactions between agents and roads. In addition to LSTMs, multi-head attention is exploited in Jean [14] to handle interactions between agents, but road map information is still missing. Recently, TPCN [15] and DCMS [16] introduce techniques from point cloud processing to learn scenario representation. They employ a spatial module to extract features of waypoints as well as map information and a temporal module to capture sequential information of agents. Besides, several transformer based models [17]–[19] utilize a stack of self-attention and cross-attention modules to capture complex interactions across agents, road lines, and temporal states, in a decoupled way. Multipath++ [1] designs a multi-context gating, an efficient variant of cross-attention, to fuse various interactions and further employs ensemble to improve the multimodality of predictions.

Alternatively, graph neural networks (GNNs) have recently attended much attention in the field of motion forecasting with graph data capturing the sparse and irregular topology of road networks efficiently. For example, Vectornet [7] proposes a two-level graph neural network to produce vectorized representation of scenario components. A local graph network extracts features of each component, including trajectories of agents and road polygons, and global interactions between these objects are further processed with another graph convolution layer. Based on the representation from Vectornet, TNT [20] designs a goal-based prediction decoder, and DensenTNT [21] further improves the goal prediction module with a dense goal candidate set. However, the topology of road networks is not effectively exploited in Vectornet with a fully-connected global graph. To address it, LaneGCN [8] models road networks with lane graphs and designs a graph convolutional network to capture the complex topology of lane graphs. Similarly, Gohome [10] and THOMAS [22] encode the structure of road networks with the help of lanelet-level graphs and output a heatmap to predict positions of agents. Furthermore, LaneRCNN [9] proposes an agent-specific subgraph to combine historical

motions of agents and their respective local contexts, and handles interactions through pooling in the global lane graph. In addition to lane graphs, HEAT [11] employs heterogeneous graphs to model various agent-agent interactions.

In contrast with these methods, we propose a dynamic heterogeneous graph to represent dynamic scenarios including agents and road networks, instead of a static lane-graph for road networks [8]–[10]. Furthermore, we design a novel heterogeneous graph convolutional recurrent network to address the heterogeneity in nodes and edges of a graph and capture its time-varying topology and signal.

III. NOTIONS AND PRELIMINARIES

Notions. In this paper, we represent a discrete-time dynamic graph and its discrete snapshots with \mathcal{G} and $\mathcal{G}_p = \{\mathcal{V}_p, \mathcal{E}_p\}_{p=1}^P$, and use the subscript p to indicate terms belonging to the p -th snapshot \mathcal{G}_p . Specifically, \mathcal{V}_p indicates vertex set and \mathcal{E}_p is edge set. The topology of \mathcal{G}_p is represented by adjacency matrix A_p , and signals or features on nodes in the graph are denoted as X_p , with $\mathbf{x}_{p,i} = x_p(v_i)$ corresponding to features of node $v_i \in \mathcal{V}_p$ and $X_p = [\mathbf{x}_{p,1}, \mathbf{x}_{p,2}, \dots, \mathbf{x}_{p,n}]^T$, $n = |\mathcal{V}_p|$. If the graph is further heterogeneous, we use superscripts to distinguish different types. For example, the set of vertices is $\mathcal{V}_p = \bigcup_z \mathcal{V}_p^z$ and the set of edges is $\mathcal{E}_p = \bigcup_r \mathcal{E}_p^r$, with \mathcal{V}_p^z and \mathcal{E}_p^r indicating different types of node sets and edge sets. X_p^z as a sub-matrix of X_p indicates features of nodes $v_i^{z_i} \in \mathcal{V}_p^z$. Besides, matrices and vectors are generally represented by capital letters and bold lowercase letters.

A. Graph Convolution

Convolution has been generalized from Euclidean data to graph data to enable deep neural networks to capture the irregular topology of graphs recently. Generally, the definition of graph convolution derives from either spectral graph theory or message passing strategies, corresponding to spectral graph convolutional networks [23]–[26] and spatial graph convolutional networks [27]–[30]. Spatial graph convolutional networks are much prevalent with their flexible and diverse designs of message passing and aggregation schemes. They generally consist of two stages, message passing in neighborhoods and node feature update. For each node $v_i \in \mathcal{V}$, features on its neighbors $v_j \in N(v_i)$ are first processed with an aggregator function \square to generate a message $msg(v_i)$, node v_i then updates its features based on the message from its neighbors and its previous layer representation $x_l(v_i)$.

$$msg(v_i) = \square_{v_j \in N(v_i)} \varphi(x_l(v_j), x_l(v_i)) \quad (1)$$

$$x_{l+1}(v_i) = \xi(x_l(v_i), msg(v_i)), \quad (2)$$

where $x_l(v_i)$ indicates the feature of node v_i in the l -th layer of graph neural networks, $\varphi(\cdot)$ and $\xi(\cdot)$ represent message functions and update functions, respectively.

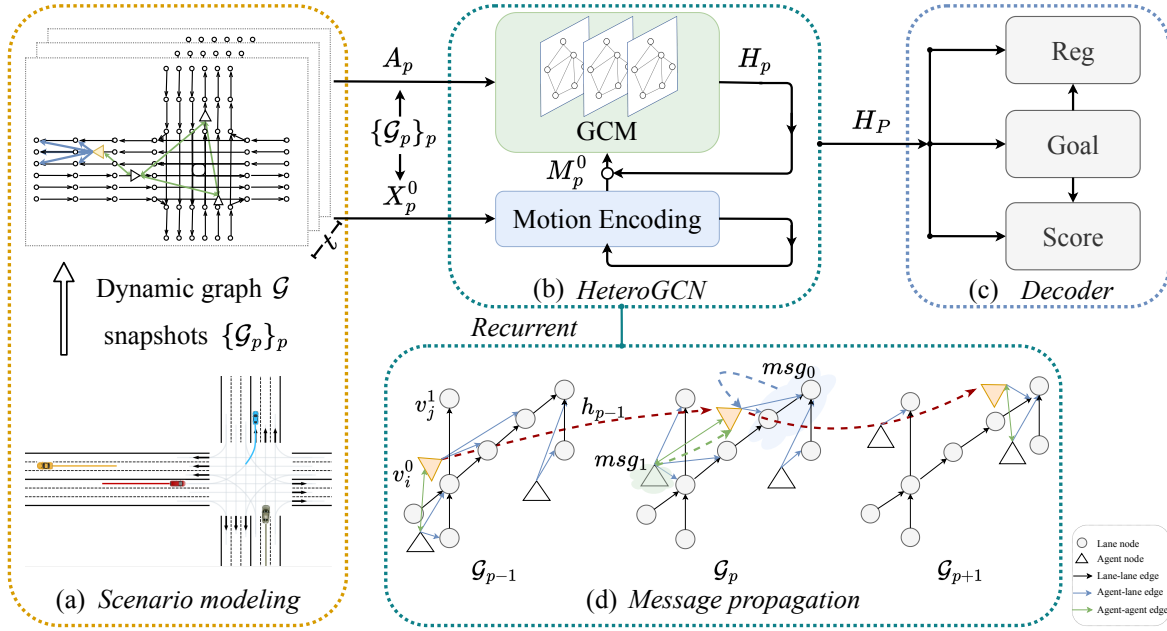


Fig. 2. Illustration of the framework. The dynamic graph for scenario modeling is demonstrated with a randomly selected agent (yellow triangle) in (a). Specifically, agent nodes and lane nodes are respectively represented as triangles and circles, and various interactions between them are indicated by edges in different colors. Based on the dynamic graph, the proposed heterogeneous graph convolutional recurrent network further captures high-order information of scenarios and forecasts future trajectories of agents, as shown in (b) and (c). Specially, message passing strategies for dynamic graphs in HeteroGCN are demonstrated in (d), with various colored dashed lines indicating message propagation along different types of edges.

IV. DYNAMIC GRAPHS FOR SCENE MODELING

We exploit dynamic graphs to explicitly model driving scenarios and their evolution over time. Specially, all of the scenario components, including agents and roads, and their multi-type interactions are jointly encoded in the topology of graphs.

Given a sequence of historical scenes, we first group them every τ discrete time, and construct a snapshot for each group instead of per discrete time to reduce computation. In other words, the p -th snapshot \mathcal{G}_p is built with information at time $t = \tau * (p - 1) - T' + 1, \tau * (p - 1) - T' + 2, \dots, \tau * p - T'$, with $T' = \tau * P$ and $p = 1, 2, \dots, P$. Due to the diversity of scenario components and their interactions, each snapshot is constructed as a *heterogeneous* graph.

Specifically, we consider two kinds of nodes *i.e.*, agents and lane segments, and four kinds of edges, including \langle agent, agent \rangle , \langle agent, lane \rangle , \langle lane, agent \rangle , and \langle lane, lane \rangle , in graphs. Without loss of generality, we assume that the set of vertices \mathcal{V}_p keeps the same in different \mathcal{G}_p , except their attributes vary with p . For the sake of clarity, we omit the subscript p of nodes below, when without causing confusion.

Nodes. We take each agent in the scenario as an agent node $v_i^0 \in \mathcal{V}^0$, and each lane segment as a lane node $v_j^1 \in \mathcal{V}^1$. Agent node features are designed as their states and state displacements. Specifically, for the p -th group of historical scenes, there are τ discrete locations and displacements per agent node $v_i^0 \in \mathcal{V}_p$, at time $t = \tau * (p - 1) - T' + 1, \tau * (p - 1) - T' + 2, \dots, \tau * p - T'$, and we adopt its state at $t = \tau * p - T'$, *i.e.*, $s_{\tau * p - T'}(v_i^0)$, and all the displacements

between these τ adjacent states as agent node features $x_{p,i}^0 = x_p(v_i^0)$ in \mathcal{G}_p , $p = 1, 2, \dots, P$. Similarly, the features of lane nodes are initially adopted from their locations and location displacements, and the features are further processed with a two-layer graph convolutional network, a variant of GraphSage [29], to encode map topologies.

Lane-lane edges (\mathcal{E}^0) are linked following the topology of road networks. Specifically, if lane segment v_i^1 and segment v_j^1 are directly connected in sequence according to the road direction, a directed edge $e_{i,j}^0 = \langle v_i^1, v_j^1 \rangle \in \mathcal{E}^0$ is constructed to connect v_i^1 to v_j^1 . Since road topology is static, \mathcal{E}^0 is the same in different \mathcal{G}_p and the subscript p is omitted.

Lane-agent edges (\mathcal{E}^1) are built on lane-lane edges \mathcal{E}^0 . Specially, we encode *the speed, heading, and location of agents* at corresponding time into the topology of \mathcal{G}_p . Specifically, for historical scenes at time $t = \tau * (p - 1) - T' + 1, \tau * (p - 1) - T' + 2, \dots, \tau * p - T'$, we first find the k nearest lane nodes for each agent node v_i^0 based on its coordinate $c_{p,i} = c_t(v_i^0)$, $t = \tau * p - T'$, and discard some of them belonging to opposing lanes.¹ Then, starting from these nodes, we perform a depth-first-search (DFS) along edges in \mathcal{E}^0 , exploring as far as possible until all nodes reachable from the source node within the maximum depth have been found. The maximum depth of DFS is based on the average speed of the agent, the average gap between adjacent lane nodes, and the time to forecast. Finally, we link the agent node v_i^0 to the explored lane nodes $\{v_j^1\}_j$ with edges $\mathcal{E}_p^1 = \{e_{i,j}^1 = \langle v_i^0, v_j^1 \rangle\}$. Meanwhile, we obtain

¹On intersections, we keep all k nodes, considering that agents may make a U-turn.

agent-lane edges $\mathcal{E}_p^2 = \{e_{j,i}^2 = \langle v_j^1, v_i^0 \rangle \mid \forall e_{i,j}^1 \in \mathcal{E}_p^1\}$.

Agent-agent edges are constructed in accordance with the distance between their locations. Specifically, the distance between v_i^0 and v_j^0 is computed with the ℓ_1 norm to approximate the distance of agents along roads.

$$d_p(v_i^0, v_j^0) = \|c_p(v_i^0) - c_p(v_j^0)\|_1, \quad p = 1, 2, \dots, P. \quad (3)$$

Then, they are connected with direct edges $e_{i,j}^3, e_{j,i}^3 \in \mathcal{E}_p^3$ in \mathcal{G}_p , if $d_p(v_i^0, v_j^0) < \delta_{aa}$, with δ_{aa} as a hyperparameter denoting the distance threshold.

V. HETEROGENEOUS GRAPH CONVOLUTIONAL RECURRENT NETWORKS

We first outline the framework of the proposed graph neural networks, then elaborate its components and introduce the learning procedure.

A. Framework

As presented in Fig. 2, the whole framework consists of an encoder to learn vectorized representations of dynamic scenarios and their components and a decoder to produce future trajectories of agents.

The encoder is designed as a heterogeneous graph convolutional recurrent network. It takes in dynamic scenarios that are modeled as dynamic graphs and aggregates spatio-temporal information of dynamic graphs with a graph convolution module (GCM) and a motion encoding module. For each snapshot \mathcal{G}_p , $p = 1, 2, \dots, P$, the motion encoding module as a causal module produces motion features M_p^0 for each agent node from its historical trajectory. The motion features M_p^0 together with spatial features H_{p-1}^0 from \mathcal{G}_{p-1} are then processed with a spatio-temporal gate $g(\cdot)$ to update the features of agent nodes at the beginning of the graph convolution module,

$$H_{p-1}^0 \leftarrow g(H_{p-1}^0, M_p^0), \quad p = 1, 2, \dots, P, \quad (4)$$

with H_0^0 initialized as a zero matrix. As an example, $g(\cdot)$ is implemented as summation in this paper. A stack of heterogeneous graph convolution operators in the GCM further aggregate information to processes complex high-order interactions in snapshots \mathcal{G}_p .

$$H_p = GCM(H_{p-1}, A_p), \quad p = 1, 2, \dots, P, \quad (5)$$

with features of lane nodes initialized as map features $H_0^1 = X_1^1$. Notably, the encoder is a recurrent network and the GCM is shared across different snapshots $\{\mathcal{G}_p\}_{p=1}^P$ of \mathcal{G} .

Based on encoded representation H_P from the encoder, the decoder composed of three branches further predicts K goals $\{\hat{s}_T^k\}$, future trajectories $\hat{S}_f^k = [\hat{s}_1, \hat{s}_2, \dots, \hat{s}_{T-1}]$, $k = 1, 2, \dots, K$, and their corresponding confidence scores, respectively.

B. Motion Encoding Module

The motion encoding module aims to extract motion features of agents from their raw trajectory features $\{X_1^0, X_2^0, \dots, X_p^0\}$. Specifically, two 2-layer multilayer perceptrons (MLPs) first map the raw agent features X_p^0 , positions and displacements, in each snapshot \mathcal{G}_p into feature spaces and produce corresponding embeddings. Notably, these MLPs are common to different snapshots. Taking in these two embedding sequences, two 1-layer GRUs further process information across snapshots, respectively. Finally, a linear layer fuses the features corresponding to positions and displacements from respective GRUs to obtain motion features M_p^0 , $p = 1, 2, \dots, P$.

C. Heterogeneous Graph Convolution Operator

To represent various nodes and capture their multiple relationships, we design a heterogeneous graph convolution operator through message passing. For the sake of clarity, we ignore the subscript p of items in this subsection.

Generally, we adopt different message passing schemes along distinct types of edges in \mathcal{G} . For any node $v_i^{z_i}$, messages msg_r to $v_i^{z_i}$ are first aggregated within each of its distinct neighborhoods $\{N^r(v_i^{z_i})\}_r$, $r = 0, 1, \dots, 3$, and these messages are further combined and processed to produce its context representation $msg(v_i^{z_i}) \in \mathbb{R}^d$, with d indicating the number of node hidden features.

$$msg(v_i^{z_i}) = \text{ReLU}\left(\sum_r \max_{v_j \in N^r} msg_r(v_j^{z_j} \rightarrow v_i^{z_i})\right), \quad (6)$$

$$z_i, z_j \in \{0, 1\} \text{ and } r = 0, 1, \dots, 3.$$

Along each type of edges, the message from $v_j^{z_j}$ to $v_i^{z_i}$ is defined as a function of node feature $\mathbf{h}_j \in \mathbb{R}^d$ ($H = [\mathbf{h}_1, \dots, \mathbf{h}_j, \dots, \mathbf{h}_n]^T \in \mathbb{R}^{n \times d}$) and its relationship $r(v_i^{z_i}, v_j^{z_j}) \in \mathbb{R}^d$ with the target node

$$msg_r(v_j^{z_j} \rightarrow v_i^{z_i}) = f(\mathbf{h}_j, r(v_i^{z_i}, v_j^{z_j})). \quad (7)$$

The $f(\cdot) : \mathbb{R}^{2d} \rightarrow \mathbb{R}^d$ is designed as an MLP in order to approximate a suitable function by learning from data. The relationship $r(v_i^{z_i}, v_j^{z_j})$ between nodes is computed based on their feature similarity and coordinate displacement

$$r(v_i^{z_i}, v_j^{z_j}) = \psi((Q_z \mathbf{h}_i) \odot \mathbf{h}_j, \mathbf{c}_i - \mathbf{c}_j), \quad (8)$$

where $\psi(\cdot)$ represents a learnable non-linear transformation, Q_z is a learnable affine matrix, $\mathbf{c}_i = c(v_i^{z_i})$ denotes node coordinates, and \odot indicates the Hadamard product.

Based on the context message $msg(v_i^{z_i})$ and a self-transformation $\nu_z(\cdot)$, the convolution operator outputs node features

$$\mathbf{h}_{p,i} = \text{ReLU}(W_{z_i} \cdot [\nu_{z_i}(\mathbf{h}_{p-1,i}) \parallel msg(v_i^{z_i})]), \quad (9)$$

$$z_i = 0, 1 \text{ and } p = 1, 2, \dots, P,$$

where $W_{z_i} \in \mathbb{R}^{d \times 2d}$ represents a learnable parameter matrix. Specially, a shortcut is further introduced to facilitate information and gradient propagation, and then Eq. (9) becomes

$$\mathbf{h}_{p,i} = \text{ReLU}(W_{z_i} \cdot [\nu_{z_i}(\mathbf{h}_{p-1,i}) \parallel msg(v_i^{z_i})] + \mathbf{h}_{p-1,i}). \quad (10)$$

TABLE I

RESULTS ON THE TESTING SET OF ARGOVERSE MOTION FORECASTING BENCHMARK (* INDICATING RESULTS WITH ENSEMBLE).

Method	$K = 1$			$K = 6$			B-minFDE
	minADE	minFDE	MR	minADE	minFDE	MR	
LaneRCNN	1.69	3.69	0.57	0.90	1.45	0.12	2.15
Jean	1.74	4.24	0.69	1.00	1.42	0.13	2.12
Prime	1.91	3.82	0.59	1.22	1.56	0.12	2.10
LaneGCN	1.71	3.78	0.59	0.87	1.36	0.16	2.05
Gohome	1.69	3.65	0.57	0.94	1.45	0.10	1.98
DenseTNT(minFDE)	1.68	3.63	0.58	0.88	1.28	0.13	1.98
THOMAS	1.67	3.59	0.56	0.94	1.44	0.10	1.97
SceneTransformer	1.81	4.06	0.59	0.80	1.23	0.13	1.89
Home+Gohome*	1.70	3.68	0.57	0.89	1.29	0.09	1.86
Multipath++*	1.62	3.61	0.56	0.79	1.21	0.13	1.79
HeteroGCN	1.62	3.52	0.55	0.82	1.19	0.12	1.84
HeteroGCN-en*	1.57	3.41	0.54	0.79	1.16	0.12	1.75

TABLE II

RESULTS ON THE TESTING SET OF ARGOVERSE2 MOTION FORECASTING BENCHMARK (* INDICATING RESULTS WITH ENSEMBLE).

Method	$K = 1$			$K = 6$			B-minFDE
	minADE	minFDE	MR	minADE	minFDE	MR	
WIMP	3.09	7.71	0.84	1.47	2.90	0.42	-
Drivingfree	2.47	6.26	0.72	1.17	2.58	0.49	3.03
LGU	2.77	6.91	0.73	1.05	2.15	0.37	2.77
THOMAS	1.95	4.71	0.64	0.88	1.51	0.20	2.16
QML*	1.84	4.98	0.62	0.69	1.39	0.19	1.95
BANet*	1.79	4.61	0.60	0.71	1.36	0.19	1.92
HeteroGCN	1.79	4.53	0.59	0.73	1.37	0.18	2.00
HeteroGCN-en*	1.72	4.40	0.59	0.69	1.34	0.18	1.90

D. Motion Prediction Decoder

We adopt a goal-based decoder. It consists of three branches to predict K future states and their respective scores. All of these branches are designed as MLPs.

The goal branch takes in the representation of agents output by GCMs H_P^0 and predicts K goals $\{\hat{s}_T^k\}_{k=1}^K$. Then, regression branch completes the trajectories $\hat{S}_f^k = [\hat{s}_1^k, \hat{s}_2^k, \dots, \hat{s}_{T-1}^k]$ conditioned on the embedding of predicted goal \hat{s}_T^k and agent features H_P^0 , $k = 1, 2, \dots, K$. Finally, scoring branch estimates the confidence $\{\hat{q}^k\}_{k=1}^K$ of each prediction.

E. Learning

The loss function of the whole model consist of three parts, corresponding to goal prediction, trajectory completion, and score estimation, respectively.

$$\mathcal{L} = \lambda_1 \mathcal{L}_{goal} + \lambda_2 \mathcal{L}_{reg} + \lambda_3 \mathcal{L}_{score}, \quad (11)$$

with $\lambda_1, \lambda_2, \lambda_3$ as hyperparameters to balance the loss. Similar to previous methods [8], [9], we choose the smooth ℓ_1 loss $l(\cdot)$ for \mathcal{L}_{goal} and \mathcal{L}_{reg} , and the max-margin loss for \mathcal{L}_{score} . To obtain diverse predictions, \mathcal{L}_{goal} and \mathcal{L}_{reg} are computed based on the prediction achieving the minimum goal displacement error

$$\mathcal{L}_{goal} = \frac{1}{|\mathcal{V}^0|} \sum_{v_i^0 \in \mathcal{V}^0} \min_k l(\hat{s}_T^k, s_T) \quad (12)$$

$$\mathcal{L}_{reg} = \frac{1}{|\mathcal{V}^0|(T-1)} \sum_{v_i^0 \in \mathcal{V}^0} \sum_{t=1}^{T-1} l(\hat{s}_t^{k^*}, s_t), \quad (13)$$

where $\{s_t\}_{t=1}^T$ represent ground truth future states of agents and k^* indicates the index of the prediction achieving the minimum loss in Eq. (12). The max-margin loss drives the model to assign the highest confidence score to the optimal prediction $\hat{S}_f^{k^*}$. Mathematically, with ϵ indicating the margin,

$$\mathcal{L}_{score} = \frac{1}{|\mathcal{V}^0|(K-1)} \sum_{v_i^0 \in \mathcal{V}^0} \sum_{k \neq k^*} \max(\hat{q}^k - \hat{q}^{k^*} + \epsilon, 0). \quad (14)$$

VI. EXPERIMENTAL RESULTS

We evaluate our model on the public Argoverse and Argoverse2 Motion Forecasting benchmarks, where the proposed model achieves significant improvements over a collection of state-of-the-art published methods. Furthermore, several ablation studies are conducted to verify the proposed modules.

A. Experimental Settings

Datasets. Argoverse [31] consists of 324,557 scenarios which are split into training, validation, and testing sets with the ratio 205,942 : 39,472 : 78,143. The scenarios are generally selected from challenging cases, including interactions, turns, lane changes, and dense traffic. Each scenario contains the locations of objects in 5 seconds sampled at 10 HZ, where initial 2 seconds (20 frames, $-T_{19}, \dots, T_0$) are adopted as observations to forecast the trajectory in the

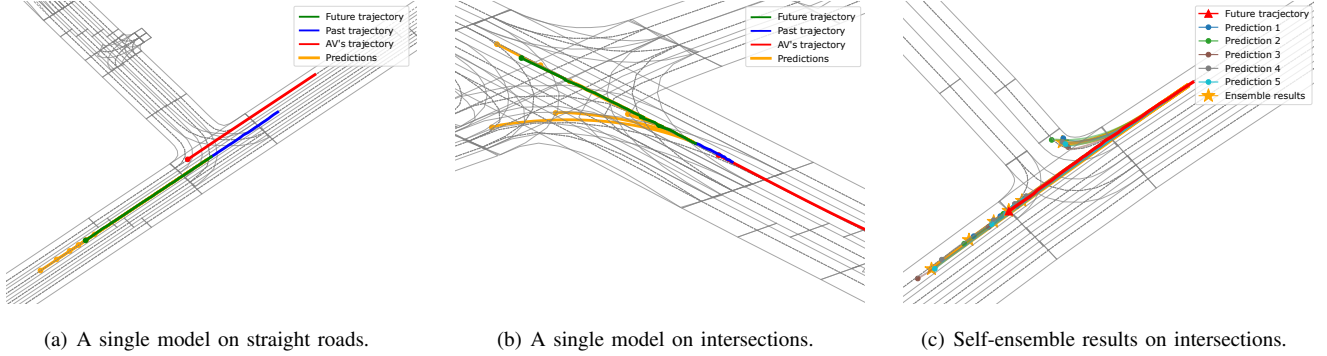


Fig. 3. Illustration of prediction results on the validation set of Argoverse. For clarity, trajectories of surrounding vehicles are not presented and self-ensemble is illustrated with five models.

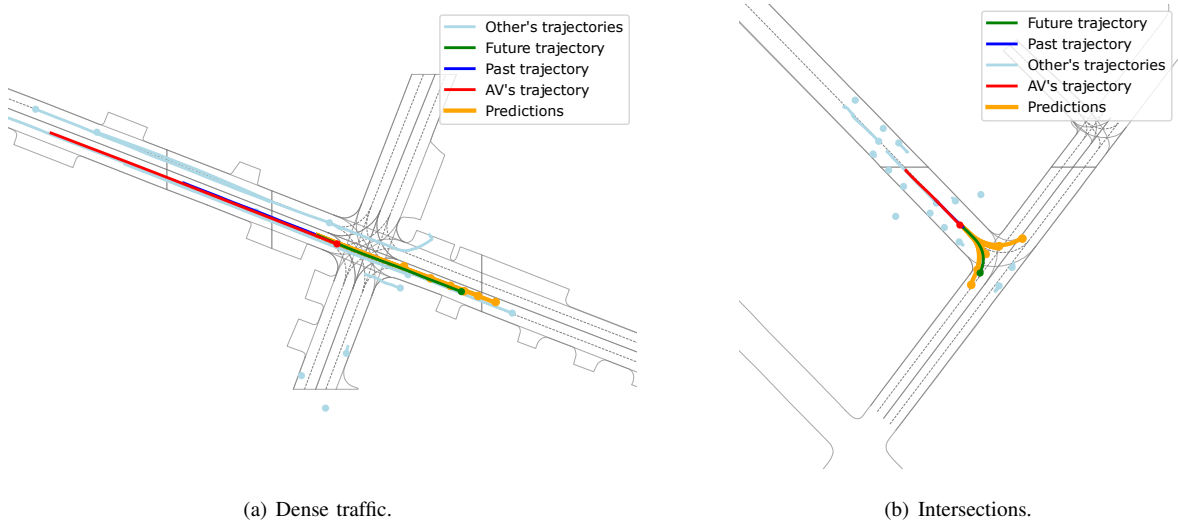


Fig. 4. Illustration of prediction results on the validation set of Argoverse2.

next 3 seconds (30 frames, T_1, \dots, T_{30}). A case typically consists of multiple moving agents, including an autonomous vehicle (AV) and other cars, and a single “interesting” agent is selected to predict per sequence. Locations of agents are provided as their states $\{s_t\}$ and HD maps are also rendered.

Besides, Argoverse2 [32] provides more challenging data with a longer forecast horizon, predicting 6 seconds based on 5 second observations, than Argoverse. It contains 250,000 scenarios with a split ratio of 8:1:1 for training, validation, and testing sets. Furthermore, compared with Argoverse, Argoverse2 contains 5 rather than 1 object types, including vehicle, pedestrian, cyclist, etc., each with dynamic and static categories. Agent states are further expanded into location, velocity, orientation, and one-hot encoding of agent types.

Metrics. According to the setting of Argoverse and Argoverse2 Motion Forecasting leaderboards, we predict K trajectories for each “interesting” agent and report the following metrics: Minimum Average Displacement Error (minADE@K), Minimum Final Displacement Error (minFDE@K), Miss Rate (MR@K), Brier minimum Final Displacement Error (B-minFDE@K), with $K = 1$ and 6. ADE is the averaged ℓ_2 -norm distance between the prediction

and the ground truth over all the time steps, and minADE@K refers to the minimum of K predictions. Similarly, the minFDE@K represents the minimum ℓ_2 -norm distance between the prediction of final position (goal) and the ground truth. Based on minFDE@K, MR@K is defined as the ratio of scenarios where the minFDE@K is beyond 2 meters. Finally, the B-minFDE@K further considers the probability of the optimal prediction.

Configurations. We adopt a scenario-wise coordinate system in the experiments, that is, all agents in the scenario share the same coordinate system. We take the location of the agent to predict at $t = 0$ as the origin, and adopt its current direction as x -axis. All the data are normalized accordingly. In graph construction, historical states $S_h = [s_{-T'+1}, s_{-T'+2}, \dots, s_0]$ are sliced into P groups with interval $\tau = 5$, *i.e.*, $P = 4$ in Argoverse and $P = 10$ in Argoverse2. The $\psi(\cdot)$ and the $\nu(\cdot)$ in the graph convolution operator each use a linear layer followed by a ReLU activation function. The GCM contains 2 and 3 graph convolution operators for Argoverse and Argoverse2, respectively. Models are trained with the Adam [33] optimizer with batch size 128 for 40 and 90 epochs on Argoverse and Argoverse2.

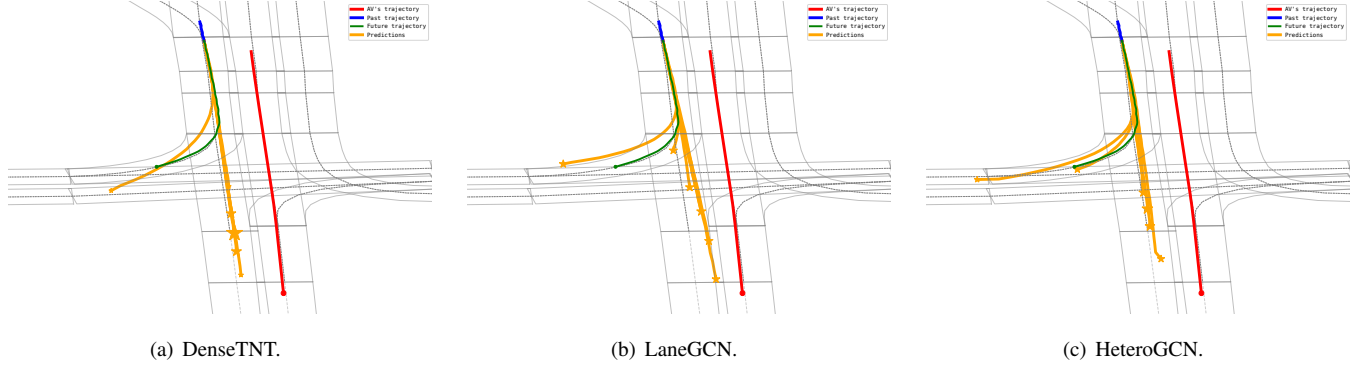


Fig. 5. Comparison of prediction results on the validation set of Argoverse using respective official code of baselines, with the goal of each predicted trajectory represented by a pentagram and its size indicating the confidence. For clarity, trajectories of surrounding vehicles are not presented.

Baselines. We compare with a collection of state-of-the-art methods in motion forecasting. First, **Prime** [34] exploits a model-based generator and a learning-based evaluator to produce feasible future trajectories. Besides, **Jean** [14] employs LSTMs and multi-head attention to handle trajectories of agents and their interactions. Then, a series of GNNs based methods are compared. **LaneGCN** [8] builds a lane graph for HD maps and captures various interactions through additional attention modules, and **BANet** [35] as a variant further fuses lane boundary information. Similarly, **Gohome** [10] and **THOMAS** [22] exploit a lanelet-level graph to encode HD map. **LaneRCNN** [9] further adopts agent-specific graphs and realizes interaction through pooling in the global lane graph. Besides, social interactions are processed with graph-based attention in **WIMP** [36]. **DenseTNT** [21] relies on the scenario representation of Vectornet, a two-level graph, and generates trajectories from dense goal candidates. Furthermore, **SceneTransformer** [17] directly takes in sequence data and exploits transformers to handle interactions via factorized attention. Finally, **Multipath++** [1] proposes a context gating module to handle interactions and employs model ensemble to enhance performance.

B. Results and Analysis

As presented in Table I and Table II, the proposed method outperforms all the baseline models in terms of B-minFDE@6, the official ranking metric on Argoverse and Argoverse 2. It still performs the best in accordance with most other metrics like minFDE. As presented in Fig. 3 and Fig. 4, the predicted trajectories of HeteroGCN are realistic and diverse on both Argoverse and Argoverse2. HeteroGCN adopting dynamic graphs for scenario modeling achieves significant improvements over static road graph based methods, like LaneGCN, LaneRCNN, GoHome, and THOMAS. Compared with VectorNet and DenseTNT, the proposed model further takes into account the heterogeneity and evolution of nodes and edges, and effectively captures the topology of roads. In contrast with SceneTransformer, HeteroGCN explicitly encodes various interactions with graphs rather than implicitly through factorized attention, which facilitates

the deep models to exploit high-order relationships between nodes. As shown in Fig. 5, HeteroGCN produces more accurate predictions than baselines.

Following previous methods [1], [35], we further employ a self-ensemble strategy to enhance the robustness and accuracy of prediction. With a tiny disturbance on the network architecture and hyper-parameters, we obtain eight submodels of the proposed method. Then the k -means algorithm is employed to cluster the produced states from these models into 6 categories. The centers of the generated clusters are adopted as final predictions and their confidence scores are obtained by aggregating the initial scores of trajectories within respective clusters. As presented in Table I and Table II, the proposed HeteroGCN-en performs the best among baselines with respective ensemble strategies, such as Multipath++ and BANet.

C. Ablation Studies

Ablations on scenario modeling. In order to evaluate the benefits of scenario modeling with dynamic heterogeneous graphs, we study the following variants.

- **HomoGCN** ignores the heterogeneity in nodes and edges in GCMs. It is achieved by taking a common message passing scheme and transformation for different z and r in Sec. V-C.
- **HeteroGCN-static** employs a static graph \mathcal{G} , *i.e.*, a common graph topology \mathcal{A} for all the graph convolution layers. Motion encoding module remains to process all of the historical trajectories. The first GCM directly takes in the final hidden state from motion encoding module as agent node features (lane node features are the same as HeteroGCN), and following GCMs feed on the output of preceding GCMs to fuse road and agent information. Others are the same as HeteroGCN.
- **HomoGCN-static** further ignores the heterogeneity in nodes and edges in GCMs, compared with HeteroGCN-static.

As presented in Table III, compared with the baseline variant HeteroGCN-static that models scenarios as homogeneous static graphs and exploits a homogeneous version

TABLE III
ABLATION STUDIES OF SCENARIO MODELING ON THE TESTING SET OF ARGOVERSE2.

Ablation variants	Heterogeneous	Dynamic	$K = 1$			$K = 6$			B-minFDE
			minADE	minFDE	MR	minADE	minFDE	MR	
HomoGCN-static			1.90	4.87	0.61	0.77	1.46	0.20	2.10
HeteroGCN-static	✓		1.84	4.67	0.61	0.74	1.40	0.18	2.04
HomoGCN		✓	1.85	4.69	0.60	0.74	1.39	0.18	2.04
HeteroGCN(proposed)	✓	✓	1.79	4.53	0.59	0.73	1.37	0.18	2.00

TABLE IV
ABLATION STUDIES OF HETEROGENEOUS GRAPH CONVOLUTIONAL RECURRENT NETWORKS ON THE TESTING SET OF ARGOVERSE2.

Motion Encoding	GCM			Recurrent	$K = 1$			$K = 6$			B-minFDE
	GCM-1	GCM-2	GCM-3		minADE	minFDE	MR	minADE	minFDE	MR	
✓				-	3.03	8.36	0.76	1.26	3.03	0.49	3.67
	✓			✓	2.02	5.05	0.63	0.80	1.50	0.20	2.14
✓	✓			✓	1.88	4.79	0.61	0.75	1.43	0.19	2.07
✓		✓		✓	1.84	4.68	0.60	0.74	1.39	0.19	2.03
✓			✓		1.85	4.71	0.61	0.75	1.41	0.19	2.06
✓			✓	✓	1.79	4.53	0.59	0.73	1.37	0.18	2.00

of the proposed GCNs, HeteroGCN-static and HomoGCN achieve better performance by further considering the heterogeneity and the evolution of scenario components and their interactions, respectively. Furthermore, considering the heterogeneity and evolution jointly, the proposed HeteroGCN performs the best.

Ablations on the main components of HeteroGCNs.

As shown in Table IV, all of the modules play a significant role in the scenario representation learning for motion forecasting. First, the motion encoding module that pre-encodes motion features of agents increases the performance from 2.14 into 2.07 in terms of B-minFDE. Furthermore, the proposed graph convolution module (GCM) effectively handles multi-type interactions in scenarios. Even with the GCM just composed of one graph convolution layer, the proposed model still outperforms all the single baselines presented in Table II. With the increment of the number of graph convolution layers in GCM from 1 to 3, the performance keeps improving. Specially, designing the network as a recurrent one, different snapshots of a dynamic graph are processed with a common GCM, saves free-parameters and reduces the B-minFDE from 2.06 to 2.00.

D. Computational Complexity and Running Time

The computational complexity of HeteroGCNs is dominated by graph convolution with $O(|\mathcal{E}|d^2)$, d indicating the dimension of node features and $\mathcal{E} = \bigcup_r \mathcal{E}^r$. In terms of running time, HeteroGCN is still competitive. The average inference time of LaneGCN, DenseTNT, and HeteroGCN is 55.32, 138.59, and 57.03 milliseconds on Argoverse with batch size 1, with their official code on a computer with an RTX 2080 GPU, respectively.

VII. CONCLUSION

In this paper, we have presented a framework to learn dynamic scenario representation and forecast future motions of agents in autonomous driving systems. First, the

proposed driving scenario modeling strategy with dynamic graphs explicitly models complex interactions like agent-road and their evolution in the scenario. Furthermore, the designed heterogeneous graph convolutional recurrent network learns to exploit multiple high-order interactions and spatio-temporal information in the scenario jointly yet differently and improves the motion forecasting performance on several challenging public benchmarks. In future, it is interesting to extend the framework from motion forecasting to motion planning.

REFERENCES

- [1] B. Varadarajan, A. Hefny, A. Srivastava, K. S. Refaat, N. Nayakanti, A. Cornman, K. Chen, B. Douillard, C. Lam, D. Anguelov, and B. Sapp, "Multipath++: Efficient information fusion and trajectory aggregation for behavior prediction," in *Proc. IEEE Int. Conf. Robot. Automat.*, Philadelphia, PA, USA, May 2022.
- [2] Y. Chai, B. Sapp, M. Bansal, and D. Anguelov, "Multipath: Multiple probabilistic anchor trajectory hypotheses for behavior prediction," in *3rd Annu. Conf. Robot Learn.*, Osaka, Japan, October 2019.
- [3] H. Cui, V. Radosavljevic, F.-C. Chou, T.-H. Lin, T. Nguyen, T.-K. Huang, J. Schneider, and N. Djuric, "Multimodal trajectory predictions for autonomous driving using deep convolutional networks," in *Proc. IEEE Int. Conf. Robot. Automat.*, Montreal, QC, Canada, May 2019.
- [4] M. Bansal, A. Krizhevsky, and A. Ogale, "Chauffeurnet: Learning to drive by imitating the best and synthesizing the worst," in *Robot.: Sci. Syst.*, Freiburg im Breisgau, Germany, June 2019.
- [5] S. Casas, W. Luo, and R. Urtasun, "Intentnet: Learning to predict intention from raw sensor data," in *2nd Annu. Conf. Robot Learn.*, Zürich, Switzerland, October 2018.
- [6] J. Hong, B. Sapp, and J. Philbin, "Rules of the road: Predicting driving behavior with a convolutional model of semantic interactions," in *IEEE Conf. Comput. Vis. Pattern Recognit.*, 2019.
- [7] J. Gao, C. Sun, H. Zhao, Y. Shen, D. Anguelov, C. Li, and C. Schmid, "Vectornet: Encoding hd maps and agent dynamics from vectorized representation," in *IEEE Conf. Comput. Vis. Pattern Recognit.*, 2020.
- [8] M. Liang, B. Yang, R. Hu, Y. Chen, R. Liao, S. Feng, and R. Urtasun, "Learning lane graph representations for motion forecasting," in *Proc. Eur. Conf. Comput. Vis.*, Glasgow, UK, August 2020.
- [9] W. Zeng, M. Liang, R. Liao, and R. Urtasun, "LaneRCNN: Distributed representations for graph-centric motion forecasting," in *Proc. Int. Conf. Intell. Robots Syst.*, Prague, Czech Republic, September 2021.

- [10] T. Gilles, S. Sabatini, D. Tsishkou, B. Stanciulescu, and F. Moutarde, "GOHOME: graph-oriented heatmap output for future motion estimation," in *Proc. IEEE Int. Conf. Robot. Automat.*, Philadelphia, PA, USA, May 2022.
- [11] X. Mo, Z. Huang, Y. Xing, and C. Lv, "Multi-agent trajectory prediction with heterogeneous edge-enhanced graph attention network," *IEEE Trans. Intell. Transp. Syst.*, vol. 23, no. 7, pp. 9554–9567, 2022.
- [12] A. Alahi, K. Goel, V. Ramanathan, A. Robicquet, L. Fei-Fei, and S. Savarese, "Social LSTM: Human trajectory prediction in crowded spaces," in *IEEE Conf. Comput. Vis. Pattern Recognit.*, 2016.
- [13] A. Gupta, J. Johnson, L. Fei-Fei, S. Savarese, and A. Alahi, "Social GAN: Socially acceptable trajectories with generative adversarial networks," in *IEEE Conf. Comput. Vis. Pattern Recognit.*, Salt Lake City, UT, USA, June 2018.
- [14] J. Mercat, T. Gilles, N. El Zoghby, G. Sandou, D. Beauvois, and G. P. Gil, "Multi-head attention for multi-modal joint vehicle motion forecasting," in *Proc. IEEE Int. Conf. Robot. Automat.*, Paris, France, May 2020.
- [15] M. Ye, T. Cao, and Q. Chen, "TPCN: Temporal point cloud networks for motion forecasting," in *IEEE Conf. Comput. Vis. Pattern Recognit.*, June 2021.
- [16] M. Ye, J. Xu, X. Xu, T. Cao, and Q. Chen, "DCMS: Motion forecasting with dual consistency and multi-pseudo-target supervision," *arXiv preprint arXiv:2204.05859*, 2022.
- [17] J. Ngiam, V. Vasudevan, B. Caine, Z. Zhang, H.-T. L. Chiang, J. Ling, R. Roelofs, A. Bewley, C. Liu, A. Venugopal, *et al.*, "Scene transformer: A unified architecture for predicting future trajectories of multiple agents," in *10th Int. Conf. Learn. Rep.*, April 2022.
- [18] R. Girgis, F. Golemo, F. Codevilla, M. Weiss, J. A. D'Souza, S. E. Kahou, F. Heide, and C. Pal, "Latent variable sequential set transformers for joint multi-agent motion prediction," in *10th Int. Conf. Learn. Rep.*, Virtual Event, April 2022.
- [19] Z. Zhou, L. Ye, J. Wang, K. Wu, and K. Lu, "Hivt: Hierarchical vector transformer for multi-agent motion prediction," in *IEEE Conf. Comput. Vis. Pattern Recognit.*, New Orleans, LA, USA, June 2022.
- [20] H. Zhao, J. Gao, T. Lan, C. Sun, B. Sapp, B. Varadarajan, Y. Shen, Y. Shen, Y. Chai, C. Schmid, *et al.*, "TNT: target-driven trajectory prediction," in *4th Proc. Conf. Robot Learn.*, November 2020.
- [21] J. Gu, C. Sun, and H. Zhao, "Densetnt: End-to-end trajectory prediction from dense goal sets," in *IEEE Int. Conf. Comput. Vis.*, Montreal, QC, Canada, October 2021.
- [22] T. Gilles, S. Sabatini, D. Tsishkou, B. Stanciulescu, and F. Moutarde, "THOMAS: Trajectory heatmap output with learned multi-agent sampling," in *10th Int. Conf. Learn. Rep.*, Virtual Event, April 2022.
- [23] J. Bruna, W. Zaremba, A. Szlam, and Y. LeCun, "Spectral networks and locally connected networks on graphs," in *2nd Int. Conf. Learn. Rep.*, Banff, AB, Canada, Apr. 2014.
- [24] M. Defferrard, X. Bresson, and P. Vandergheynst, "Convolutional neural networks on graphs with fast localized spectral filtering," in *Adv. Neural Inf. Process. Syst.* 29, Barcelona, Spain, Dec. 2016.
- [25] R. Khasanova and P. Frossard, "Graph-based isometry invariant representation learning," in *Proc. 34th Int. Conf. Mach. Learn.*, Sydney, NSW, Australia, Aug. 2017.
- [26] F. M. Bianchi, D. Grattarola, L. Livi, and C. Alippi, "Graph neural networks with convolutional ARMA filters," *IEEE Trans. Pattern Anal. Mach. Intell.*, 2021, early access.
- [27] J. Gilmer, S. S. Schoenholz, P. F. Riley, O. Vinyals, and G. E. Dahl, "Neural message passing for quantum chemistry," in *Proc. 34th Int. Conf. Mach. Learn.*, Sydney, NSW, Australia, Aug. 2017.
- [28] P. Veličković *et al.*, "Graph attention networks," in *6th Int. Conf. Learn. Rep.*, Vancouver, BC, Canada, May 2018.
- [29] W. Hamilton, Z. Ying, and J. Leskovec, "Inductive representation learning on large graphs," in *Adv. Neural Inf. Process. Syst.*, Long Beach, CA, USA, December 2017.
- [30] K. Xu, W. Hu, J. Leskovec, and S. Jegelka, "How powerful are graph neural networks?" in *7th Int. Conf. Learn. Rep.*, New Orleans, LA, USA, May 2019.
- [31] M.-F. Chang, J. Lambert, P. Sangkloy, *et al.*, "Argoverse: 3d tracking and forecasting with rich maps," in *IEEE Conf. Comput. Vis. Pattern Recognit.*, 2019.
- [32] B. Wilson, W. Qi, T. Agarwal, J. Lambert, J. Singh, S. Khandelwal, B. Pan, R. Kumar, A. Hartnett, J. K. Pontes, *et al.*, "Argoverse 2: Next generation datasets for self-driving perception and forecasting," in *35th Adv. Neural Inf. Process. Syst., Datasets and Benchmarks Track*, 2021.
- [33] D. P. Kingma and J. Ba, "Adam: A method for stochastic optimization," in *3rd Int. Conf. Learn. Rep.*, San Diego, CA, USA, May 2015.
- [34] H. Song, D. Luan, W. Ding, M. Y. Wang, and Q. Chen, "Learning to predict vehicle trajectories with model-based planning," in *Proc. Conf. Robot Learn.*, London, UK, November 2021.
- [35] C. Zhang, H. Sun, C. Chen, and Y. Guo, "BANet: Motion Forecasting with boundary aware network," *arXiv preprint arXiv:2206.07934*, 2022.
- [36] S. Khandelwal, W. Qi, J. Singh, A. Hartnett, and D. Ramanan, "What-if motion prediction for autonomous driving," *arXiv preprint arXiv:2008.10587*, 2020.